

---

# RPU-1 “Reliant”

## Design Report

January 2025



# Table of Contents

---

- **Statement of Purpose**
- **Engine Design**
  - Propellants
  - Chamber Specifications
  - Injector Selection
  - Manufacturing
- **Test Stand Design**
  - Structural Layout
  - Piping and Instrumentation Diagram
  - Systems and Control
  - Emergency Operation
- **Safety and Testing**
  - Testing Plan Summary
  - Ignition Sequence
  - Cold Flow Procedure
  - Hotfire Procedure
  - Standard Operation of RPU-1
- **Conclusion**
  - Design and Development Summary
  - Cost Analysis
  - Future Goals

## Statement of Purpose

Rensselaer Propulsion Unit One, hereafter referred to as “RPU-1”, is RPI’s first ever liquid bipropellant rocket. RPU-1 was designed as a technology demonstrator that builds the Rensselaer Spaceflight Society’s skill and familiarity with complex engineering. It will also provide a tangible case for project sponsorships and funding in the near future. Throughout its evolution, RPU-1 was entirely designed by undergraduates, representing the Spaceflight Society’s dedication to strengthening passion and knowledge of aerospace hardware among RPI students.

---

**Reese Mount** - Design and Development Lead

**Riley Dunn** - Propulsions

**Cooper Werner** - Systems

**Slater Selinger** - Fluids

**Clara Madison** - Safety

**Garrett Brooks** - Manufacturing

**Maximilian Slavik** - Chief Engineer

# Engine Design

---

## Propellants

RPU-1 uses a liquid kerosene and gaseous nitrous oxide propellant scheme. Kerosene was chosen due to its commonality and ease of handling. Nitrous oxide is a standard oxidizer for amateur rocketry, since it is significantly more accessible compared to other oxidizers. Nitrous oxide is also self-pressurizing due to its low boiling point and high vapor pressure. This simplifies the feed system significantly. Rocket Propulsion Analysis (RPA), a computational combustion optimization tool, was used to identify an optimal oxidizer/fuel ratio of 7.938. In most small engines, the optimal ratio is not used due to thermal shock issues. This will be discussed further in later sections. The thermodynamic properties of combustion through the nozzle at this ratio are shown in [Fig. N].

Thermodynamic properties (O/F=7.938)					
Parameter	Injector	Nozzle inlet	Nozzle throat	Nozzle exit	Unit
Pressure	2.0684	2.0684	1.1901	0.1013	MPa
Temperature	3208.8794	3208.8794	3026.1897	2190.2312	K
Enthalpy	1094.5472	1094.5472	558.9594	-1402.9693	kJ/kg
Entropy	9.9382	9.9382	9.9382	9.9382	kJ/(kg·K)
Internal energy	91.1733	91.1733	-376.4652	-2059.4351	kJ/kg
Specific heat (p=const)	4.0936	4.0936	3.8441	1.7338	kJ/(kg·K)
Specific heat (V=const)	3.5061	3.5061	3.3069	1.4227	kJ/(kg·K)
Gamma	1.1676	1.1676	1.1625	1.2187	

Fig. N: Thermodynamic Properties throughout the Chamber

Brass piping for the nitrous feed line was necessary to mitigate the risk of friction autoignition. Since chamber pressure is significantly lower than vapor pressure, the risk of multiphase flow during standard operating temperatures is negligible. However,

since gaseous nitrous oxide is compressible, the feed system still required ample calculation through control volume analysis, and may require tuning during tests to alleviate the onset of small deviations from predicted flow rates. This was factored into feed system design as detailed in later sections.

## Chamber Specifications

### Chamber Pressure

As chamber pressure increases, the exhaust velocity, which is proportional to specific impulse, also increases, as shown in [Eq. N]

$$v_e = \sqrt{\frac{TR}{M} \cdot \frac{2\gamma}{\gamma - 1} \cdot \left[ 1 - \left( \frac{p_e}{p} \right)^{\frac{\gamma-1}{\gamma}} \right]}$$

Eq. N: Exhaust velocity as a function of chamber pressure p, exit pressure pe, ratio of specific heats  $\gamma$ , gas temperature T, ideal gas constant R, and molar mass M.

Preventing backflow into the injector manifold is a matter of finding a balance in pressure difference across the manifold. For most liquid engines at this scale, the stiffness [Eq. N], must be greater than 30%. The balance of manifold pressure differences can be simplified to identifying a stiffness that minimizes pressure oscillations in the injector. Note that chamber pressure is effectively a function of feed pressure, which allows the stiffness to be tuned using only one parameter without changing engine geometry. However, every engine must be optimized around an expected chamber pressure. Due to a limited budget, solenoids and pressure transducer operational tolerances constrained maximum feedline pressure to 500 psi. Adding a safety factor to MEOP yields a chamber pressure of 300 psi, a standard for small liquid rockets.

$$\text{stiffness} = (\text{feed pressure} - \text{chamber pressure}) / (\text{chamber pressure})$$

**Eq. N:** Approximate stiffness of a pressure fed cycle

## Mass Fraction and Thermal Effects

Operating RPU-1 at the optimal mass fraction yields incredibly high temperatures (3209 K). However, since this engine is meant for ground tests only, the mass of the thrust chamber assembly (TCA) was not a primary concern, allowing us to use a graphite sleeve that acts as a heat sink due to graphite's extremely high thermal inertia. Graphite is also relatively inexpensive as a cooling method, and significantly more accessible than regenerative cooling, ablative composites, or an external heat exchanger. *Siemens Simcenter 3D Thermal/Flow* was used to analyze the effects of optimal combustion temperatures on the TCA. Both nonlinear transient heat transfer simulations and steady-state hand calculations were performed using a factor of safety of 1.4 on the heat transfer coefficient. The results of this simulation for a ten second continuous hotfire are shown in [Fig. N] with a maximum temperature of 1237.67 K.

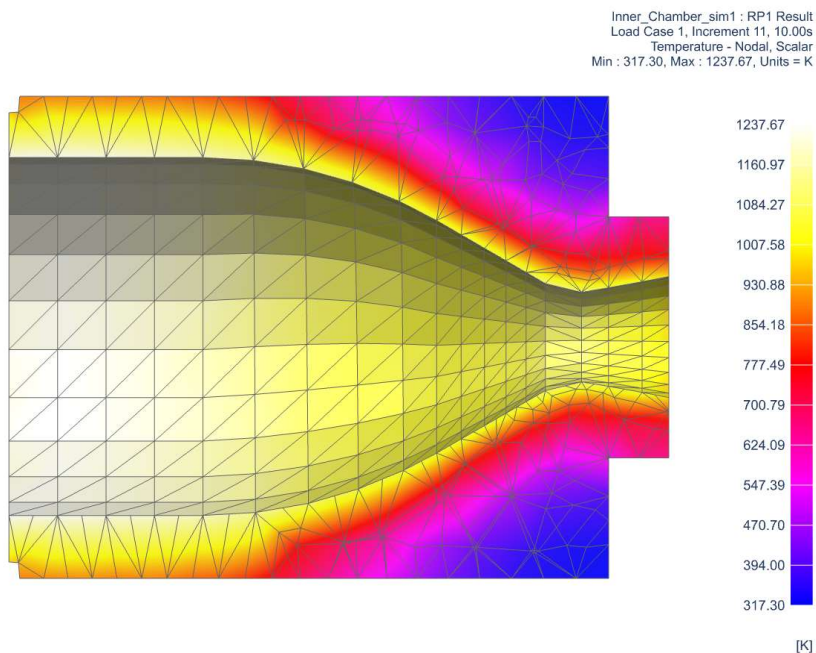
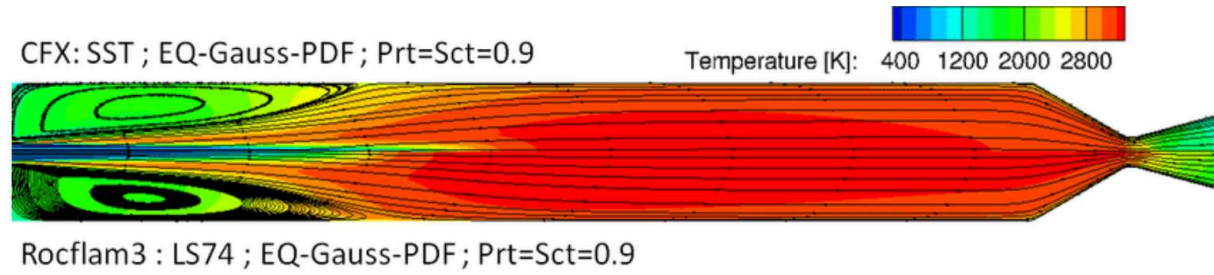


Fig. N: Ten second transient simulation of graphite insert, to analyze thermal tolerances of the TCA

This simulation does not account for large turbulent phenomena close to the impingement points near the top of the TCA. This turbulent flow pattern is very common in many different TCA designs, so it was assumed that RPU-1 will exhibit these phenomena. During an actual hotfire, these turbulent zones will carry the heat away from the injector face and towards the throat (Fig. N and Fig. N).



Rocflam3 : LS74 ; EQ-Gauss-PDF ; Prt=Sct=0.9

Fig. N: Rocflam3 Simulation data of a general TCA design; note the low-temperature circulation zones near the injector.

Despite these turbulent conditions preventing heat localization at the injector, stainless steel 304 (as opposed to aluminum 6061) was chosen for the interface component of the manifold, to ensure that long duration hotfires do not deform the injector geometry.

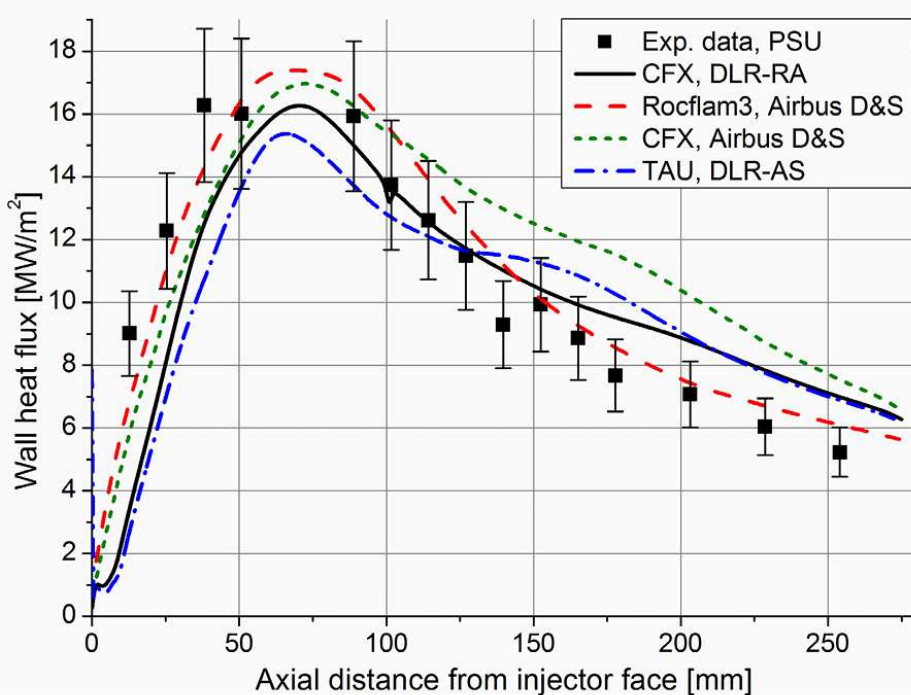


Figure 7. Comparison of the results of work [14] (black line) with experimental data [13] and simulation results of other groups [15].

Fig. N: Heat flux data demonstrating the effects of turbulent circulation zones distributing heat throughout the chamber

## Chamber Geometry

Optimized chamber geometry is provided through RPA's numerical design optimization tool. Selection of an extruded graphite rod as the TCA thermal insert provided an economic way to reach higher efficiency, as continuous cuts can be made. As a function of chamber pressure, mass fraction, and overall mass flow rate, the geometry is outlined in [Fig. N].

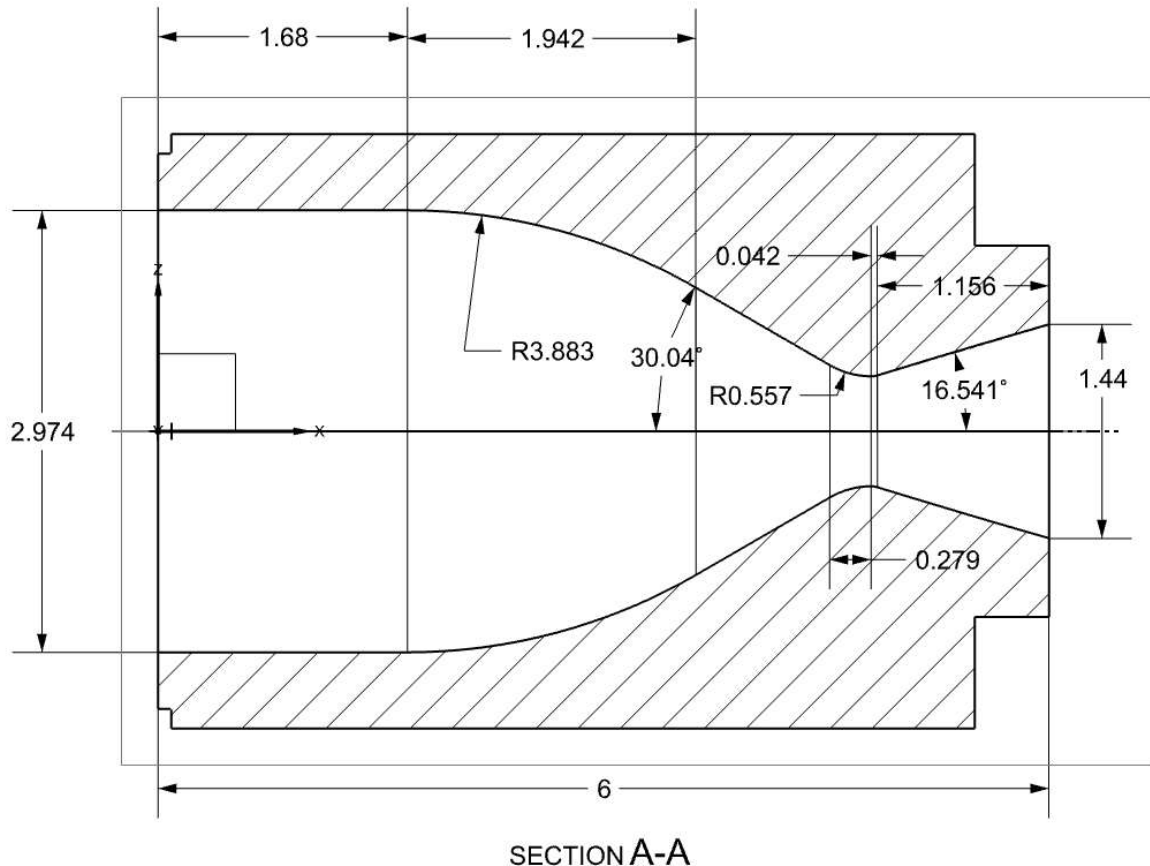


Fig. N: Extruded graphite TCA insert, displaying the precise geometry made possible by using a graphite insert.

## Injector Selection

### Principal Injector Trade Study

Since the nitrous oxide is being fed into the combustion chamber below its vapor pressure, it will be atomized when it enters. Therefore, the breakup of the kerosene stream was considered the first priority. Three types of injectors were considered for RPU-1: pintle, doublet impinging, and triplet impinging.

Pintle		Doublet	Triplet	
FoM	Weight	Pintle	Doublet	Triplet
Efficiency	0.4	0	1	-1
Manufacturability	0.4	-1	0	1
Cost	0.2	1	1	1
Total Score		-0.2	0.6	0.2

**Fig. N:** Decision matrix used in selecting RPU-1's injector

TCA dimensions heavily constrained manufacturing of the injector, especially with our limited access to specialized tooling required for drilling extremely small orifices. While a pintle provides a commonly used solution to orifice manufacturing by concentrating fabrication effort towards one small component, it is substantially harder to control during a hotfire, and taking advantage of all benefits of a pintle may even require a separate pneumatic system. Additionally, the amount of publicly available research on gaseous pintle streams is sparse. On the other hand, there have been extensive studies done on impinging gaseous injectors, mainly for rotating detonation engines. As shown in [Fig. N], a doublet impinging injector provided the optimal balance between efficiency, manufacturability, and cost.

## Doublet Impingement Analysis

RPU-1's injector plate is sized for one ring of doublet impinging injectors. Eight doublets surround the center of the chamber with nitrous oxide entering with inward radial momentum from the outer ring and kerosene impinging into it from the center [Fig. N].

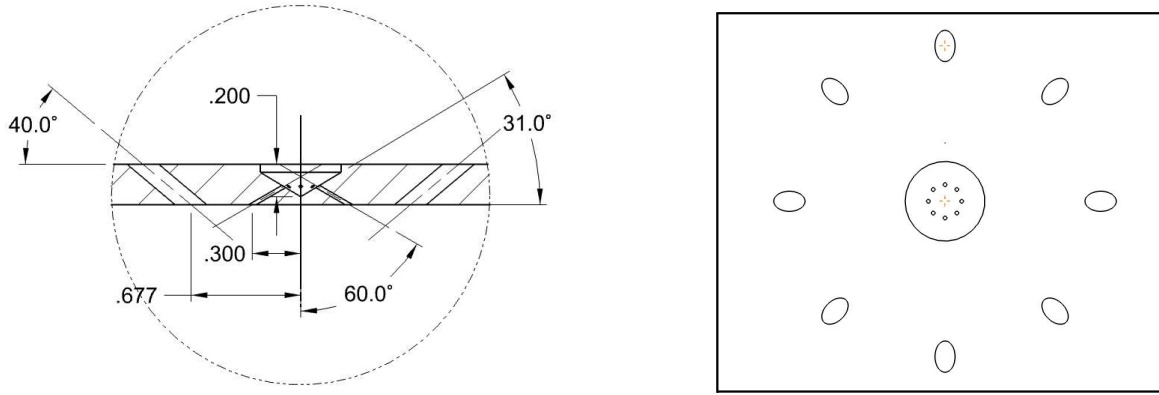
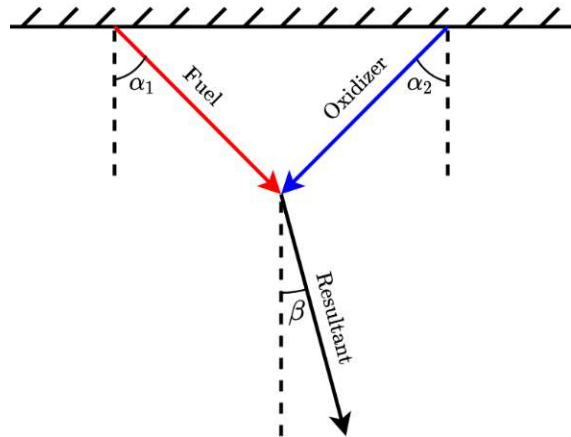


Fig. N: Schematic showing the outer nitrous ring and the kerosene inlet

The momentum of the nitrous stream is significantly greater than that of the kerosene stream, which leads to the resultant stream depending almost entirely on the nitrous inlet's orientation. {Eq. N} was used to determine the angle  $\beta$  of the resultant stream, with angles clarified by [Fig. N]. Note that for clarity in the equation, variables are denoted with f and ox to denote 1 and 2 respectively.

$$\beta = \arctan \left( \frac{m_f v_f \sin(\alpha_f) - m_{ox} v_{ox} \sin(\alpha_{ox})}{m_f v_f \cos(\alpha_f) + m_{ox} v_{ox} \cos(\alpha_{ox})} \right)$$

**Eq. N:** Resultant angle of doublet impinging streams



**Fig. N:** Display of angles corresponding to Eq. N.

RPU-1's injector is configured such that the resultant streams of the initial impingement point meet each other at a later point. Normally the resultant streams would be oriented normal to the injector face, to utilize the pressure-based momentum of unburnt propellant. However, due to our optimized propellant scheme and high momentum ratio, combined with the fact that atomization of the nitrous is guaranteed, a second impingement theoretically provides better performance by scattering the kerosene further around the injector.

## Propellant Flow and Thermochemistry

### Reaction Transition States

Nitrous Oxide and Kerosene react in an unconventional way compared to most modern rocket propellants. Instead of a single combustion reaction, N<sub>2</sub>O first decomposes into N<sub>2</sub> and Oxygen, forming a more stable configuration for some original resonance structures, which releases energy in the form of heat. Subsequently, the free oxygen reacts with long alkanes in the Kerosene mixture to produce the traditional combustion reaction. The thermochemical properties of N<sub>2</sub>O decomposition are one of the main reasons for the high O/F ratio, and using gaseous N<sub>2</sub>O theoretically provides an efficiency benefit by prioritizing the atomization of constituents that undergo a double reaction. The overall process is detailed in [Fig. N] below.

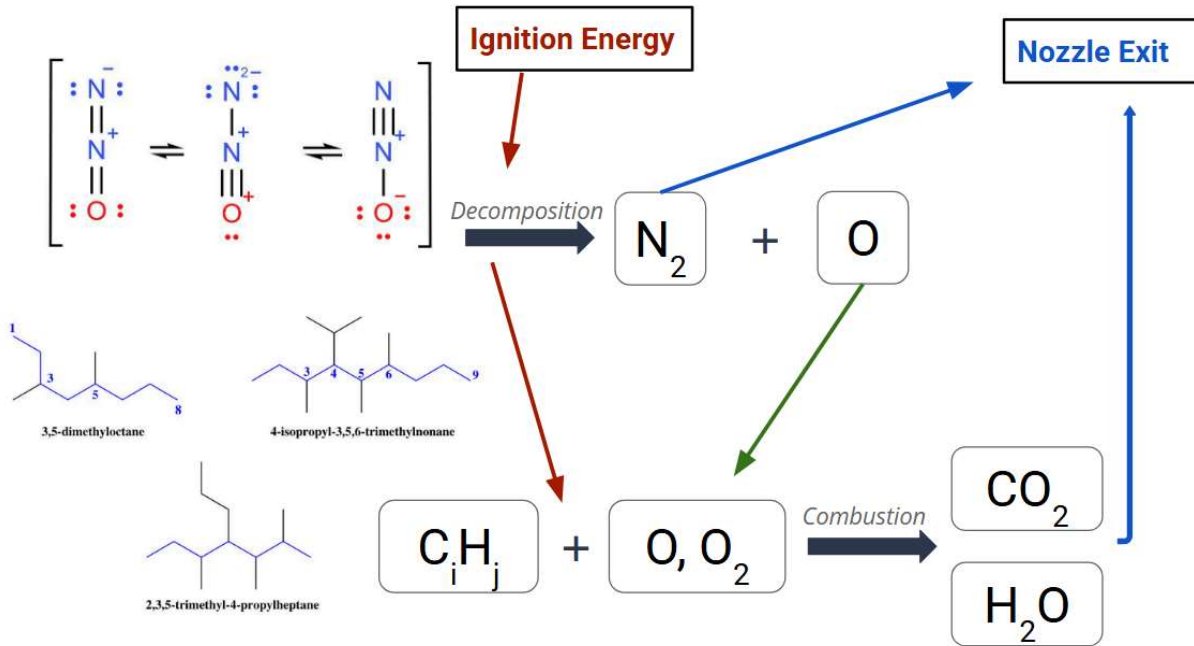


**Fig. N:** Reaction Process in RPU-1

## Oxidizer Control Volume Analysis

As mentioned in earlier sections, institute regulations and a limited budget prevented the use of N<sub>2</sub>O in its liquid state due to its significantly high vapor pressure. Estimation of compressible flow through the feed system with exit conditions at combustion temperatures proved rather difficult. However, a set of reasonable assumptions provided a concrete method of estimating flow rates and optimal injector geometry. Ideal gas behavior was assumed to occur, as N<sub>2</sub>O forms simple molecules with limited internal degrees of freedom. Additionally, entropy through the lines was considered to be negligible, as combustion did not happen inside the control volume boundary. Therefore, isentropic flow equations could be used to relate the initial and final states. To set up the control volume, an energy-rate balance was derived. The initial state inside the propellant tank assumed infinite area and zero velocity, a relatively common simplification, while the exit condition was the total injector manifold orifice area. The rate balance and assumption-based equations used are outlined in [Fig. N].

### Energy rate balance

$$\Delta \dot{E} = 0 = \dot{m}(h_i - h_f) + \dot{m} \frac{(v_i^2 + v_f^2)}{2}, \quad v_i = 0 \implies v_f = \sqrt{2(h_1 - h_2)}$$

Ideal gas regime and isentropic flow equations

$$\rho = \frac{P}{RT}, \quad \gamma = \frac{c_p}{c_v}, \quad \left(\frac{T_f}{T_i}\right) = \left(\frac{P_f}{P_i}\right)^{\frac{\gamma-1}{\gamma}}, \quad (h_i - h_f) = c_p(T_i - T_f)$$

**Fig. N:** Analytically solvable system gained from assumptions

*h is enthalpy, T is temperature, P is pressure, v is velocity, mdot is mass flow rate, Cp is specific heat at constant pressure, Cv is specific at constant volume, and R is the ideal gas constant of the used gas.*

In order to express the required injector orifice area in terms of the mass flow rate, the enthalpy change must be written as a function of pressure differential. This is where the assumptions outlined above are key, as the enthalpy of an ideal gas is inherently dependent upon temperature only. Since velocity at the injector is dependent upon enthalpy difference, the change in temperature forms a bridge between pressure differential and velocity. After utilizing the initial rate balance equation, the N<sub>2</sub>O injector velocity and mass flow rate can finally be expressed in terms of known variables, allowing us to optimize the injector geometry based on chamber pressure and tank pressure. A coefficient of discharge C<sub>d</sub> was added to account for friction in the lines and sharp corners in the manifold. For small orifices, C<sub>d</sub> is typically ~0.65. The derived velocity and mass flow rate equations are shown in [Fig. N].

$$v_{inj} = C_d \sqrt{2c_p T_1 \left( 1 - \left( \frac{P_c}{P_{tank}} \right)^{\frac{k-1}{k}} \right)}$$

$$\dot{m}_i = \dot{m}_f = \rho_f A_f v_f \implies \dot{m} = \left( \frac{\sqrt{2} C_d P_c A_{inj}}{R T_f} \right) \sqrt{c_p T_1 \left( 1 - \left( \frac{P_c}{P_{tank}} \right)^{\frac{k-1}{k}} \right)}$$

**Fig. N:** N<sub>2</sub>O stream velocity at injector, and mass flow rate throughout the feed system.

Note that [T]=K, [P]=Pa, [R]=J·kg<sup>-1</sup>·K<sup>-1</sup>, and [mdot]= kg·s<sup>-1</sup>

Since the fuel is liquid, we were able to use a much simpler flow equation based on the pressure differential without requiring the use of control volume analysis. This equation also factors in  $C_d$ , shown in [Fig. N].

$$A_{total} = \frac{\dot{m}}{C_d \sqrt{2\rho(P_{tank} - P_c)}}$$

**Fig. N:** Fuel orifice area optimization by pressure differential

## Feed System Uncertainties

Due to various valves having unknown flow coefficients, as well as compressibility and combustion causing multidimensional flow effects that cannot be simulated accurately with our current software, there will be unavoidable uncertainty in mass flow rates during operation. To mitigate the effects of this uncertainty, we designed the feed system to allow for modifications in backpressure. Between hotfire tests, the operators will be able to manually increase kerosene backpressure up to +90 psi, and nitrous feed pressure up to +50 psi. A decrease in backpressure can also be utilized if more drastic changes are needed. It is also worth noting that small fluctuations in mass flow rates

around the optimum point- by around  $\pm 15\%$  - do not cause major changes to combustion efficiency.

## Manufacturing

### Component Summary

RPU-1's outer casing subassembly, consisting of the lower cap, outer wall, and injector plate encloses the graphite insert such that it can be protected during transport and minimize the risk of splintering and dust. Stainless steel 304 was chosen due to its cost-effectiveness, thermal properties, and general resilience against the abrasive operating conditions inside the engine. Since the manifold is not directly exposed to combustion, and requires precise milling, aluminum 6061 was selected. Buna-N rubber O-rings were used to mitigate propellant leakage throughout high-pressure components. After each set of hotfire tests, the O-ring at the top of the graphite insert must be replaced, as there are no consumer grade O-rings that can withstand the incredibly high temperatures that occur inside the combustion chamber.  $\frac{1}{4}$ " NPT thread taps are used to link the manifold inlets to the feed system.

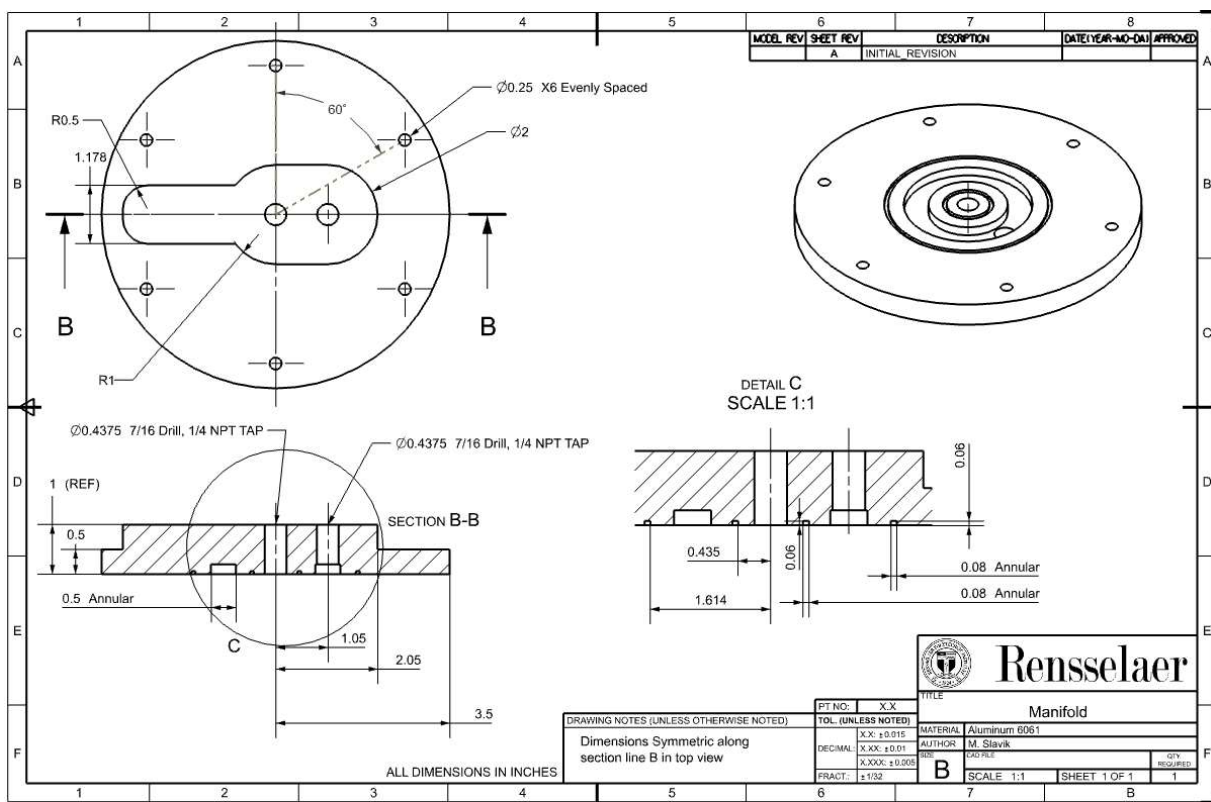
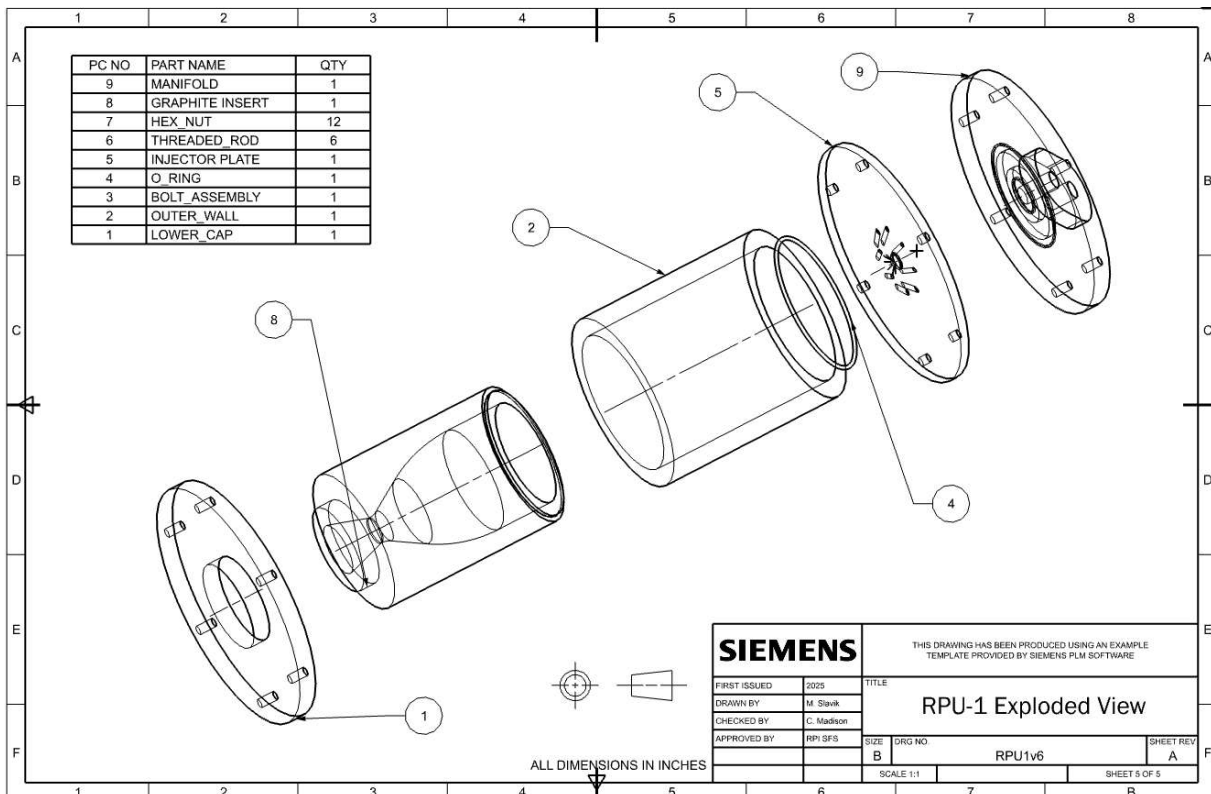
### Manufacturing Processes

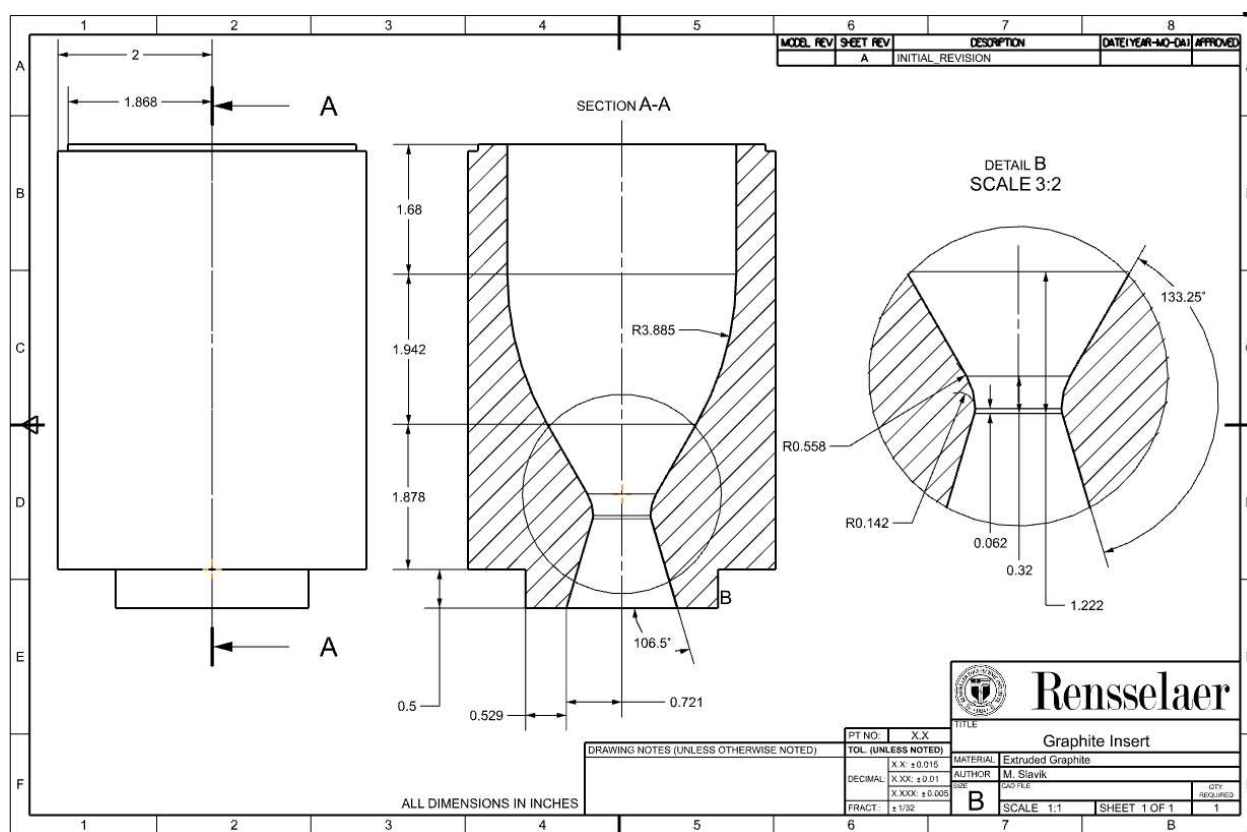
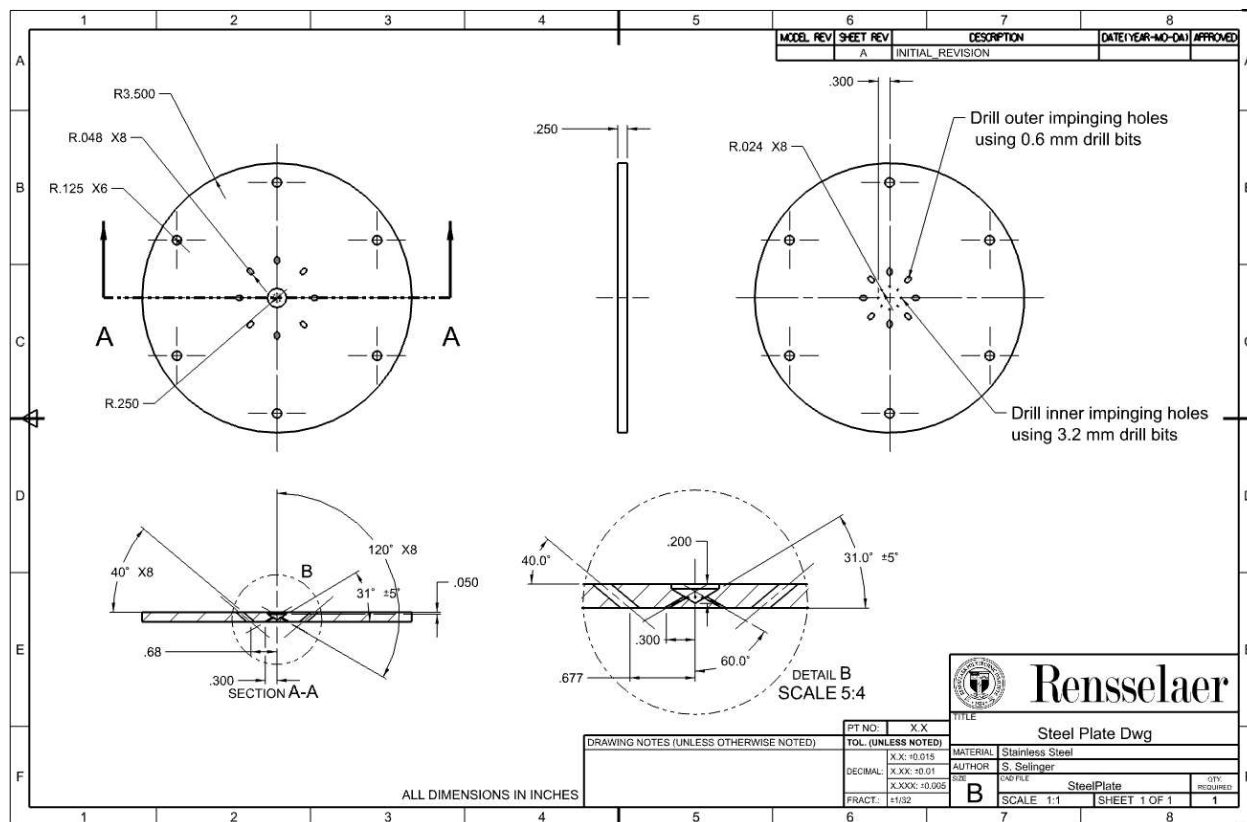
The manufacturing method for each component is detailed in [Table N]. An external machine shop was required for the injector plate and graphite rod, since they require extremely precise manufacturing and limited-access machines, such as a 4-axis mill. External manufacturing was done by the Rensselaer Machine Shop. All other components were manufactured using CNC mills, drill presses, band saws, and NPT taps from student machine shops available on campus.

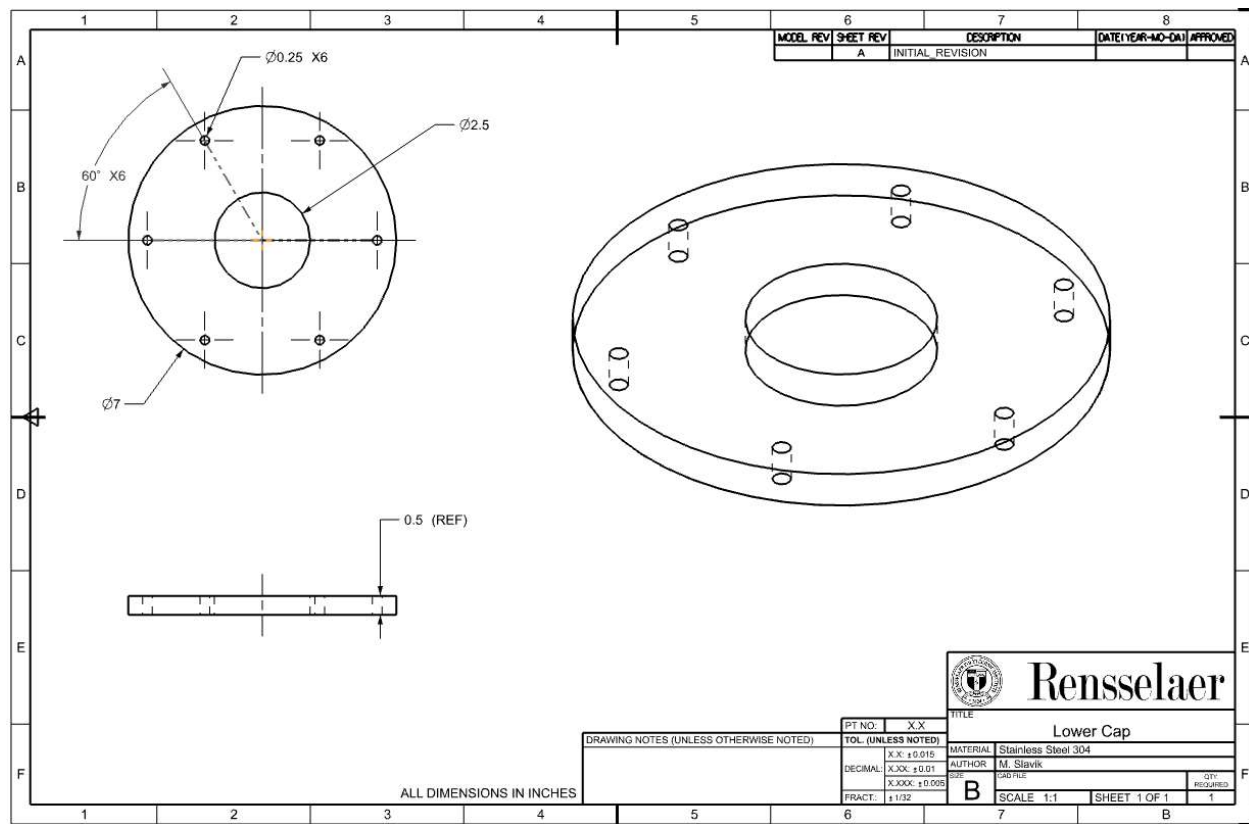
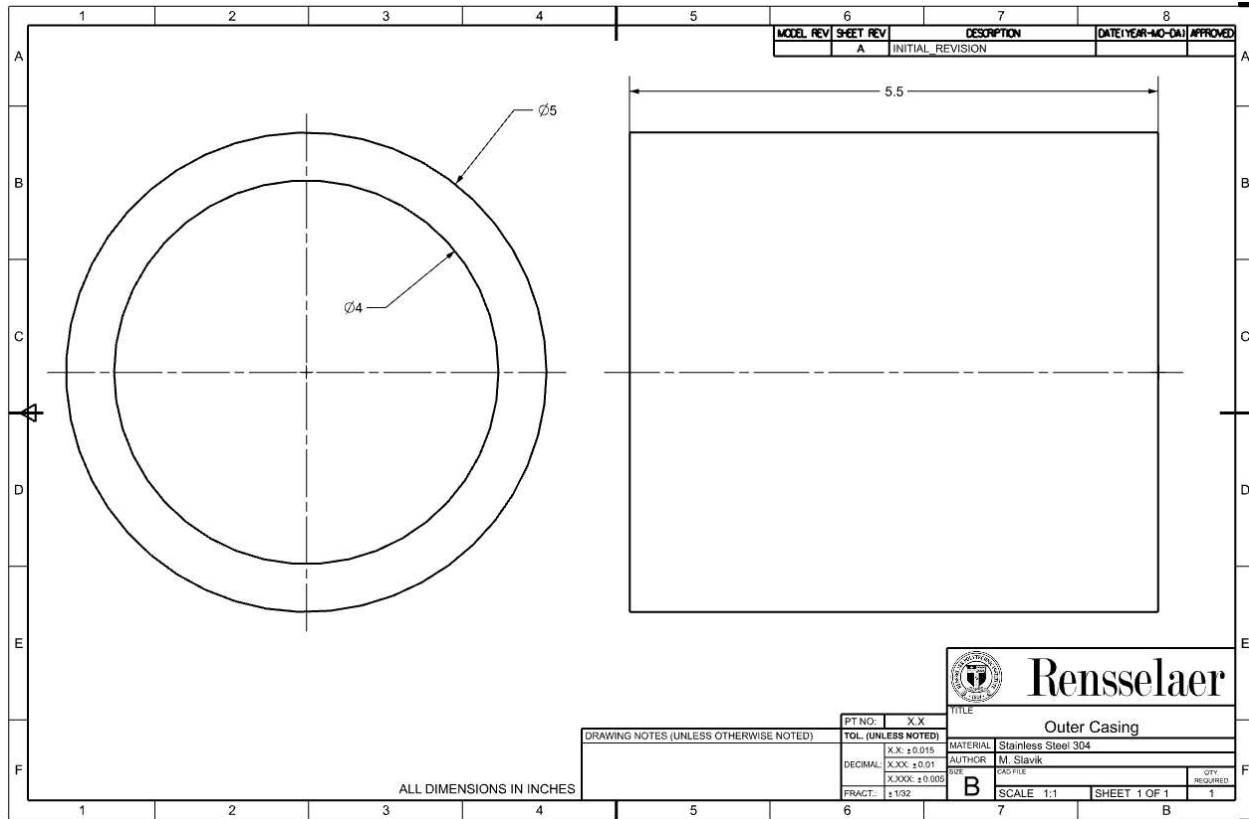
**Table N: Manufacturing Details**

Component	Material	Required Resources	Manufacturing Description
Manifold	Aluminum 6061	CNC Mill, $\frac{1}{4}$ " NPT tap	Drill mount holes, mill propellant distribution lines, drill inlet holes, tap inlet holes
Outer Wall	Stainless Steel 304	CNC Mill	Mill axially to 5.5" length
Lower Cap	Stainless Steel 304	CNC Mill	Drill mount holes, mill 2.5" dia. Center hole
Injector Plate	Stainless Steel 304	External Machine Shop	Bore center hole, drill mount holes and injector orifices
Graphite Insert	Extruded Graphite	External Machine Shop	Lathe to dimensions shown in [Fig. N]
Threaded Rods	Stainless Steel	Band Saw	Cut into six 8.5" rods

## Engine Drawing Package







# Test Stand Design

---

## Structural Layout

### General Geometry

The test stand structure primarily consists of a large aluminum 6061 0.1" thick sheet, cold-rolled steel 3mm thick L-beams ( $\sim 44\text{mm} \times \sim 36\text{mm}$ ), zinc yellow-chromate plated grade 8 steel hex screws, and grade 5 steel locknuts. The geometry consists of two rectangular prism structures such that the main structure houses everything except the engine and the smaller structure is attached to the bottom of the main frame. The engine is mounted on top of the smaller structure, separated from the pressure vessels by a thick plexiglass blast shield. The overall dimensions of the test stand frame are 45.5" x 24.75" x 24.75". There is a metal sheet bolted to the bottom of the frame that acts as the floor of the test stand. Each corner and side of the frame is secured with a bolt assembly on each plane. As pictured in the diagrams below, much of the test frame volume is empty space, even when plumbing is included. This is to allow more room for modifications and allow for easy access to engine subsystems, such as electronics and tanks. The test stand layout is clarified by [Fig. N] and [Fig. N].

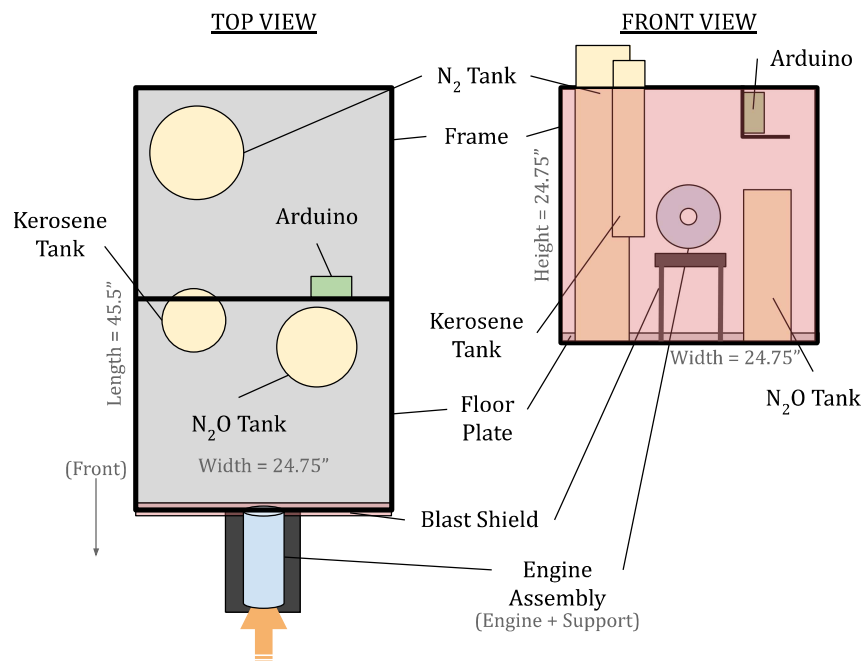


Fig. N: Test Stand Frame Diagram (Top/Front)

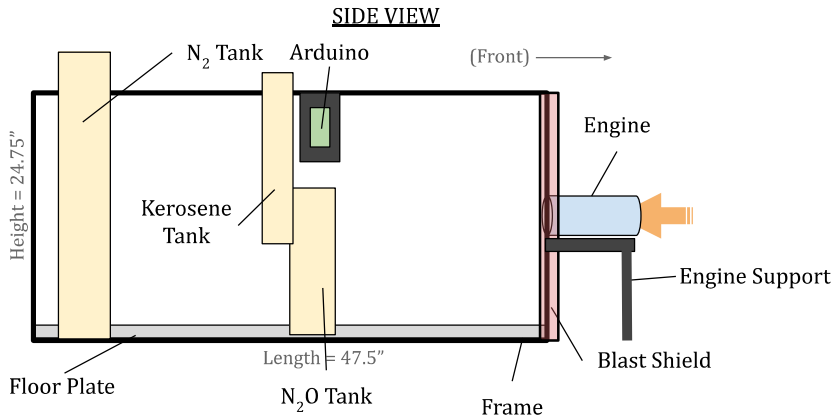


Fig. N: Test Stand Frame Diagram (Side)

## Tank Placement

Looking towards the front of the test stand (blast shield), the kerosene tank is placed inside the frame to the left, mounted between vertical L-beams and secured with straps. The nitrous tank is stored in a bucket inside the frame to the right, resting on the aluminum floor plate and surrounded by a mylar emergency blanket to limit heat transfer. The nitrogen tank also rests on the aluminum floor plate, and is placed inside the frame to the back left, strapped tightly to the corner beam.

## Engine Placement

The engine is mounted to the front end (furthest from the nitrogen tank) of the stand such that the majority of the engine sticks out from the blast shield and the pipe inlets are behind the blast shield.

## Load Cell Placement

The load cell is mounted to a support beam directly behind the engine such that the load cell is centered horizontally on the engine manifold and offset vertically towards the bottom of the engine manifold.

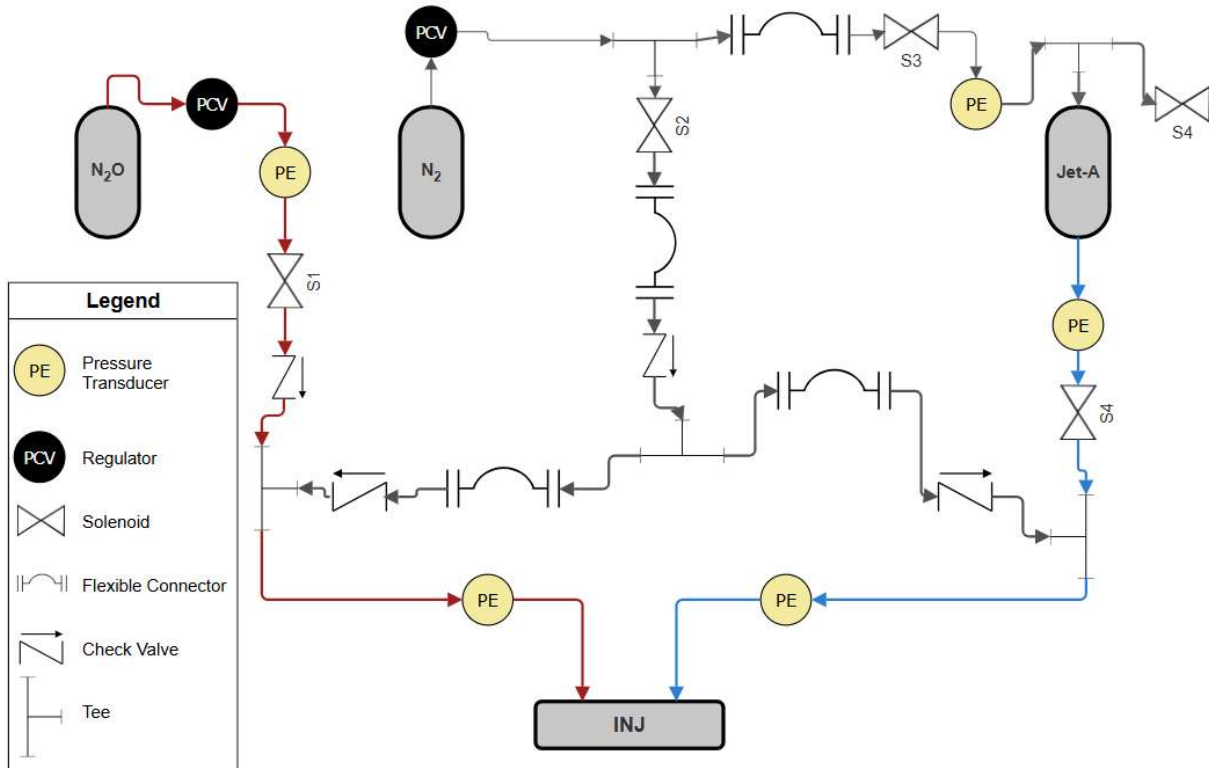
## Electronics Placement

The Arduino and PCB are housed in a 3D-printed enclosure. This enclosure is mounted on the same support beam used to mount the kerosene tank, such that the PCB hangs down and can easily connect to sensor and control assemblies throughout the test stand.

## Blast Shield

The blast shield is a plexiglass sheet that sits behind the engine with an opening that allows pipe connections. It is designed to protect critical systems within the frame in the event of a TCA Failure.

## Piping and Instrumentation Diagram



## Systems and Control

### Overview

The control system is divided into two computers that together control the engine via a system of commands. The two computers communicate with each other via wired RS485, a low bandwidth, but very long range and reliable communications protocol. In optimal conditions it can reach as far as 1100m. For our use case, we have opted for a distance of 300m accounting for the fact that vibrations from the test stand may reduce transmission distance.

The engine test stand has an arduino-based control computer, that receives commands, reads from sensors, transmits sensor data, and operates the valves and ignition source. There are a total of 10 sensors in use on RPU-1: one Load Cell, four K-Type Thermocouples, and five Pressure Transducers. We selected the HX711 load cell amplifier, AD4895 Thermocouple amplifier, and standard automotive pressure transducers for their ease of use and balance between price and precision. On each loop of the Arduino's control loop, if it has been instructed to, it will attempt to read each of the sensors. Some new data may not be collected for a given timestep, due to sampling rate limits in the sensors themselves, and in this case the most recently collected data is transmitted. This data is then compared with previously recorded data to verify safe operation of the engine, and sent to the control computer for display and logging.

## **Valve Control**

Five electrically actuated solenoid valves are used to control the flow of fuel, oxidizer, and inert gases. Each solenoid is normally closed, meaning that without power, there will be no flow. Each solenoid operates at approximately 15W, 12V @ 1.2A. The Arduino does not have the current or voltage carrying capacity for the solenoids on its own. To address this, relays are used to allow the Arduino's 5V logic level to control the flow of 12V current and thus the opening or closing of valves.

## **Control Hardware**

To link all of the electrical components in a repeatable, reliable, and fail-safe way, we have designed a printed circuit board (PCB) shield for the Arduino. This PCB has space for all the sensors, amplifiers, relays, copper traces, and screw terminals that are needed to connect each of the components. This PCB was designed in KiCAD, and was manufactured at RPI's Electrical and Computer Systems Engineering Lab.

The other computer is a standard laptop. This laptop runs a custom designed software that handles the logic, data display, and data / event logging for the engine. The software is written using Qt and C++ primarily for linux, but can be compiled on any platform. The software interfaces with a serial port opened by a USB to UART adapter, it will write commands and read data from this serial port. Sensor data is displayed and logged in the software. More details about the usage of the software can be found below in the Standard Operation of RPU-1 section.

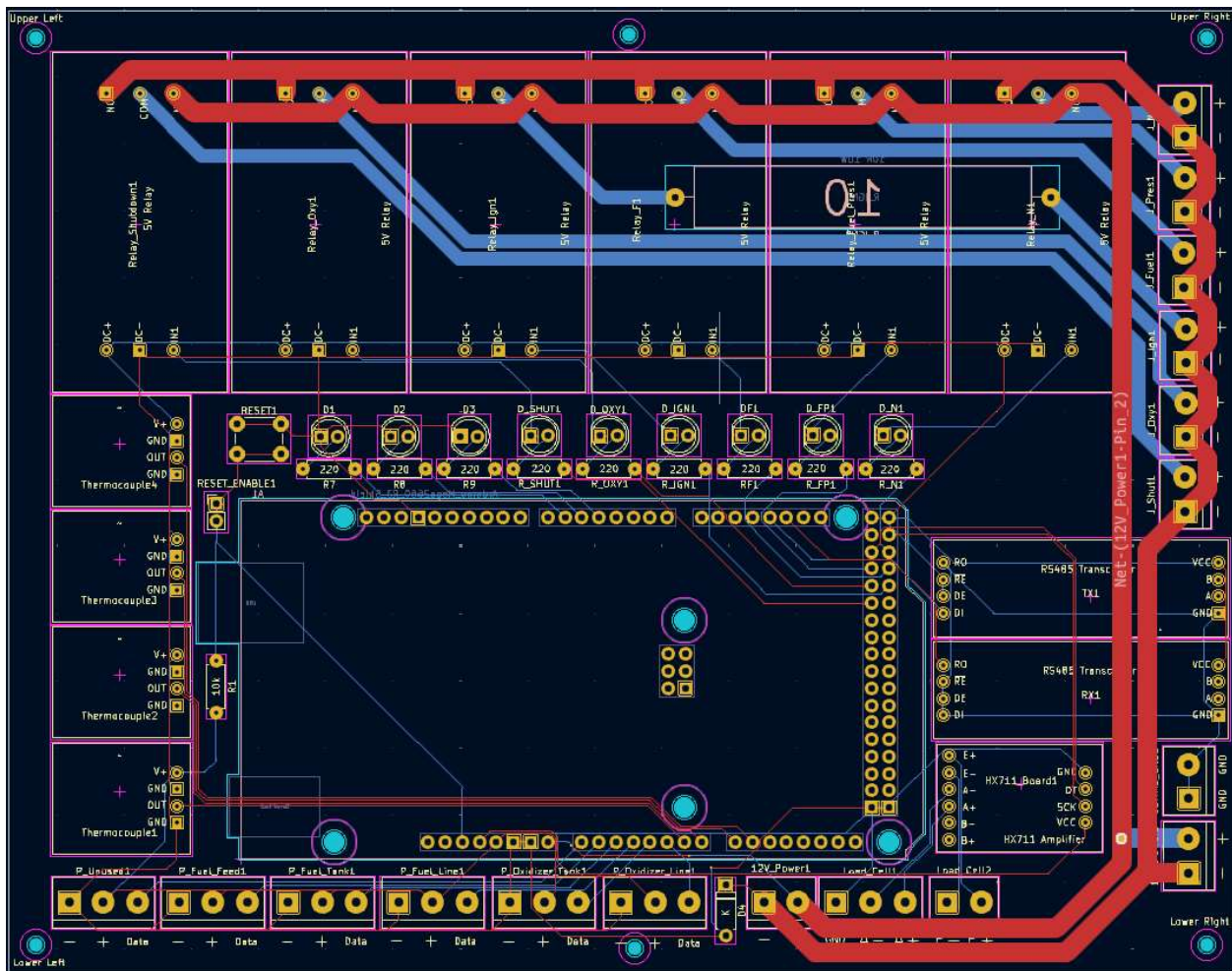


Fig N: A Diagram of the Engine Test Stand Control PCB

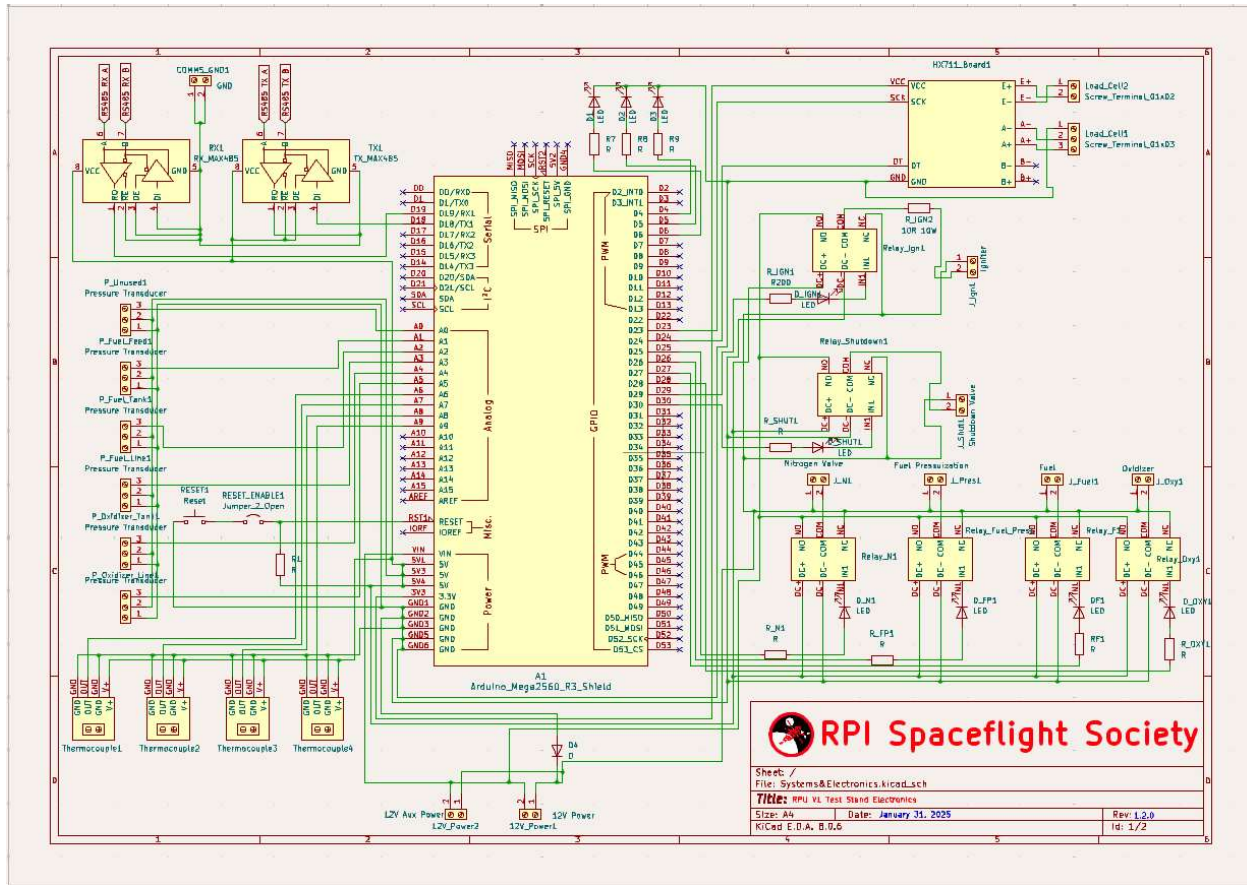


Fig N: A Wiring Diagram of the Engine Control Electronics and Sensors.

## Emergency Operation

For all rocket engines, ours included, there are a variety of failure modes that could increase the risk of damage to the engine or injury to the personnel running the engine. For that reason we have created extensive procedures, safety protocols, and electronic checks to ensure smooth and safe operation. This section describes the procedures in case of suboptimal engine performance.

## Communications Failure

RPU-1 is operated from a remote location over 750 feet away from the test stand. The safe operation of the engine requires communications to be active at all times. After the control computer and the engine computer have established a connection, they

each send a ping signal every 100ms. If either the engine computer or the control computer detect that more than 5 pings have been dropped, then both sides will start their respective shutdown processes. RPU-1 is powered by a pair of redundant batteries on the test stand. In case of power failure, all valves are normally closed with the exception of the depressurization solenoid on the kerosene tank. Once power is lost, the feed system will close and the kerosene tank will vent its pressure to atmospheric.

## **Suboptimal Engine Performance**

Both underperformance and overperformance of the engine have the possibility of damaging it. For this reason we have integrated automated checks for all of our sensors. At a rate of over one-hundred times a second the sensors are polled, and checked. Each time that sensors are polled, our code will verify that the sensor data and rate of change is in acceptable bounds. If the engine computer finds that one or more sensors are out of bounds for more than 100ms then the engine computer will initiate its shutdown procedure and indicate that to the control computer. As one last precaution, all of the data recorded by the engine computer is reported back to the control computer. This data is not only logged to disk, but is also displayed numerically and on a variety of charts. If at any time the operating personnel feel uncomfortable with the engine's performance they can trigger a countdown hold or complete shutdown of the engine with a single press of the backspace or escape keys.

## **Shutdown Procedure**

The specific shutdown procedure performed depends on the engine state. If a shutdown is triggered before the engine has opened any valves then the engine just opens the kerosene pressure relief valve to ensure there are no pressurized pipes. If only the kerosene pressurization valve has opened, then in case of shutdown, that valve is first closed, and the relief valve is opened. If either of the fuel or oxidizer valves are

opened, then upon starting the shutdown procedure all valves will close. A brief nitrogen inert flush will occur, and then the kerosene pressure relief valve will open.

# Safety and Testing

---

## Testing Plan Summary

The testing scheme for RPU-1 involves a cold flow, igniter, and hotfire in that order. Each test is detailed in the sections below.

## Cold Flow Procedure

Prior to hotfire testing, a cold flow test is planned to verify flow and sensor characteristics of the RPU-1 test stand network. To reduce all unnecessary hazards, nitrogen will be used in place of nitrous oxide and water will act as a replacement for kerosene. Due to the absence of any form of explosive danger, this test is expected to take place in the Spaceflight Society's laboratory in Ricketts 411. Though, the presence of high pressure gas cylinders will require the RPU-1 to be remotely controlled outside of the laboratory while cameras will be used for remote observation of the unit and later documentation of the test. Fig. N displays the solenoid valve configuration for the cold flow test.

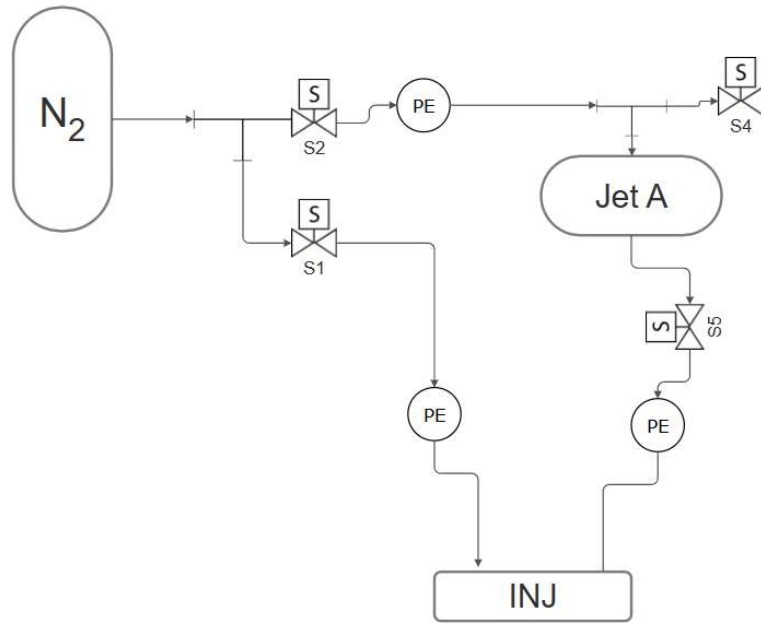


**Figure N:** Cold Flow Test Solenoid and Transducer Configuration

Following a dress rehearsal of hotfire procedures, the countdown is set from the main control computer. Solenoid valve 2 is opened to pressurize the water in the kerosene tank using nitrogen. After sufficient time is given to allow for pressurization, solenoid 5 is opened so water can flow from the kerosene tank into the injector plate for 5 seconds. Solenoid 5 is then closed. After sensor and visual verification that no leaks occurred, a second test is run. During this second test, solenoids 1 and 5 are opened simultaneously to allow both water and nitrogen to separately flow into the injector plate for 10 seconds.

## Ignitor Test Procedure

To ensure that steel wool will ignite under the expected conditions, we will measure the flame temperatures and reaction sensitivities of various amounts of steel wool under several different expected voltages. This test will be performed inside the

laboratory fume hood or outside in a controlled environment with a flame snuffer present.

## **Hotfire Assembly Procedure**

Due to the volatile nature of the propellants involved in hotfire testing, the caution exhibited during assembly and disassembly of the test stand must be on an order of magnitude higher than any test listed. Great care must be taken to ensure threads are installed properly, tanks are filled and emptied slowly and steadily, and pressurized cylinders are not jolted around. When all components arrive at the testing site, the empty stand will be placed in the testing location and staked to the ground. The engine will be attached to the blast shield and engine mount, and the load cell will be mounted flush to the manifold. Subsequently, the empty kerosene tank will be strapped into its mount using heavy duty ratchets straps, which are colored bright orange so the operators can see a strap failure from the operation site. The lower fuel control assembly consisting of a pressure transducer, solenoid, and check valve is then mounted to the bottom of the kerosene tank. Once the control assembly is in place, a braided hose is used to join the manifold inlet to the control assembly with a pressure transducer attachment next to the inlet. Once the empty kerosene tank is attached, the large nitrogen cylinder will be carefully lifted into the back of the stand and strapped tightly to the corner support. Once the assembly team is confident in the stability of the gas cylinder, the nitrogen regulator is installed and the exit pressure is calculated. Note that exit pressures on each regulator are dependent upon the conditions at the testing site, e.g. temperature, atmospheric pressure. The assembly team will not open the regulator until the test stand setup is complete. Once the nitrogen regulator is installed, the solenoid control and transducer system for the kerosene backpressure and flush lines is attached to the regulator. Following this, kerosene is gently poured into the kerosene tank via a funnel, and the main cap adapter is slowly threaded into place. The upper fuel control assembly can now be attached to the main cap adapter,

and a braided hose is used to connect the assembly to the kerosene backpressure solenoid on the nitrogen cylinder. While only fuel is present in the chamber and the nitrous oxide is stored sufficiently far away, the systems team will connect all attached pressure transducers and solenoids to the arduino controller, to minimize the assembly time when both oxidizer and fuel are present. The nitrous oxide canister, which will be wrapped in a blanket inside of a wide-base bucket to ensure it does not topple inside the stand, is wrapped with a mylar emergency blanket to mitigate heat transfer to the propellant stored inside. Once the nitrous oxide regulator is carefully attached and the required calibration is calculated based on test site conditions, the oxidizer control and sensor assembly is threaded into the regulator. The nitrogen flush line, which is assembled separately for quicker overall test stand integration, is used to attach the fuel and oxidizer lines to the nitrous flush system solenoid. The last piping component may now be attached: a braided hose and transducer subassembly that connects the oxidizer control assembly to the manifold inlet. The reset jumper wire on the PCB must be removed by the systems team, preventing an unwanted reset of the control systems while allowing quick debugging during assembly and preliminary testing. Once all sensors and valves are attached to their proper screw terminals, the systems team walks to the operation site, approximately 900-1000 feet away, while the assembly team looks over the entire test stand and double checks the quality of assembly. If the test stand is deemed safe for operation, the ignitor will carefully be placed inside the TCA and the assembly team will step back away from the stand with their PPE facing toward the pressure vessels. Once outside a 100 ft radius, the assembly team will walk toward the operation site and begin the countdown procedure.

## **Standard Operation of RPU-1**

We have developed a custom software for logging data, displaying data, and controlling the engine. This section covers how that platform works to control the engine and

handle data appropriately. The control software is written in C++ on top of the Qt UI framework. It is primarily designed to work on Linux, but should compile and be usable on all platforms. Upon starting, the software will create 3 log files: an event log that logs any important events like specific commands being sent, a data log that logs data received, and a corrupted data log, a log of any data which fails checksum verification. The user will see a screen like the one shown in Fig. N below.

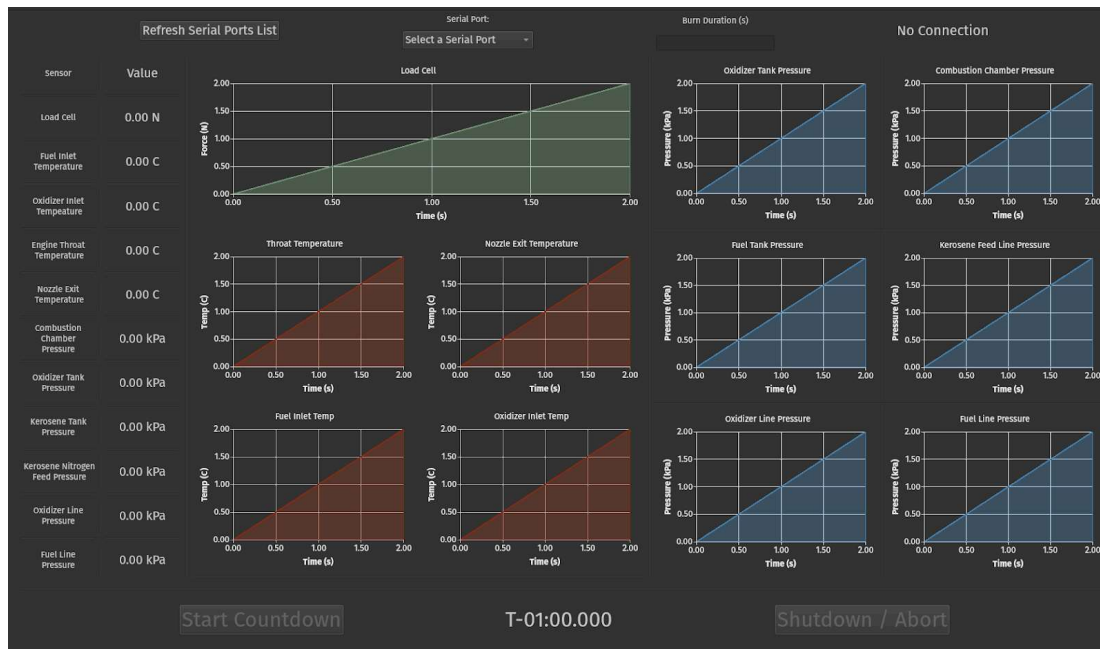


**Fig. N:** A Sample Image of the Engine Control User Interface

The control computer and the engine computer communicate over the RS485 serial protocol, the user will need to plug in a USB to UART device into the control computer. The user should then select the serial port that the USB to UART device opened from the dropdown. If the serial port is not in the dropdown, clicking the “Refresh Serial Ports List” will scan for serial devices and update the dropdown. Upon selecting the serial port, the control software will send a command to establish connection with the engine, upon successful connection, the “Start Countdown” button will become enabled. The user should then type in the desired burn duration in seconds. Afterwards

the user can press the start countdown button to start the countdown. Pressing this button also signals the engine to start logging data back to the control computer, the user will see the values for all of the engine's sensors displayed in the digital readout and on the charts. The "Shutdown" button will be enabled and display "Hold Countdown". Pressing this button will hold the countdown until the "Continue Countdown" button is pressed. Pressing the "Hold Countdown" button twice will put the engine into a safe shutdown. Upon reaching T-30s, the software will perform an automatic countdown hold that will need to be cleared by the operators who click the "Continue Countdown" button. The countdown can be held at any point before T-2s. At T-10s, the software commands the engine to perform a nitrogen gas inert flush for 3s. At T-5s, a command to open the kerosene pressurization valve is sent. At T-1.5s the ignition command is sent, the engine computer will open the fuel valve for a short burst, light the steel wool, and then open the oxidizer valve. To ensure proper ignition, the fuel valve will be opened in conjunction with the oxidizer decomposition, which is facilitated by the steel wool. After the specified burn duration, the control computer will send the shutdown command to stop the burn, run an inert gas flush, and open the kerosene depressurization valve, putting the engine into a safe state. After a successful shutdown the user will have the option to reset and prepare for another test. Throughout the duration of the burn, the engine computer will be reading the sensors and transmitting that data back to the control computer. This data will be logged in the data log and will be displayed both numerically and graphically on the control software giving the team the ability to monitor the real-time performance and analyze the performance after the test.

# Conclusion

---

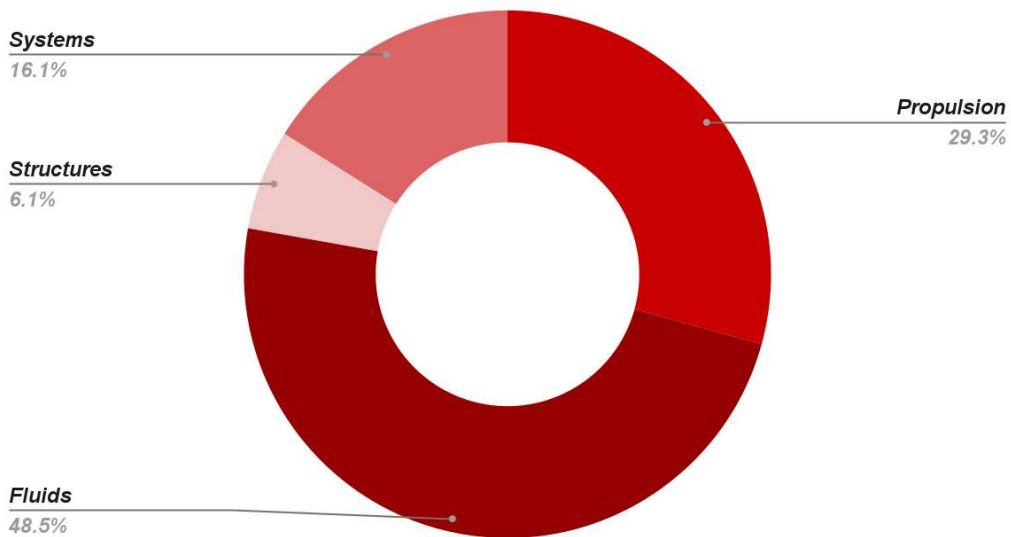
## Cost Analysis

The complete hotfire assembly contains 154 components with a total cost of \$2718 USD. On the financial scale of undergraduate rocketry, RPU-1's material cost is considerably cheap. Material costs by subcommittee are shown in [Table N].

Subcommittee	Total Material Cost
Propulsion	795.34
Fluids	1318.2
Structures	166.97
Systems	436.55
<b>TOTAL COST</b>	<b>\$2717.06</b>

Fluids connections proved to be the most expensive, with a final cost of slightly more than the propulsions hardware. For our next project, we aim to optimize the test stand such that long fluid connections are needed less frequently.

Figure N: Total Material Costs by Subcommittee



**All components directly used in the operation of RPU-1 are tabulated below:**

Component	Price per unit (\$)	Quantity	Total price (\$)	Subcommittee	Major Subassembly
Graphite Rod	112.67	1	112.67	Propulsion	Engine
½" Steel Disk	199.11	1	199.11	Propulsion	Engine
¼" Steel Disk	181.33	1	181.33	Propulsion	Engine
Steel Casing	189.95	1	189.95	Propulsion	Engine
Aluminum Disk	61.09	1	61.09	Propulsion	Engine
Washers 100pk	5.5	1	5.5	Propulsion	Engine
Nuts 50pk	2.49	1	2.49	Propulsion	Engine
Threaded Rods	13.2	1	13.2	Propulsion	Engine
TCA O-ring	20	1	20	Propulsion	Engine
Fuel O ring	5	1	5	Propulsion	Engine
Ox O ring	5	1	5	Propulsion	Engine
9ft Braided Hose	57.69	1	57.69	Fluids	Test Stand
End Connectors	17.7	12	212.4	Fluids	Test Stand
Fuel Tank Body	29.49	1	29.49	Fluids	Test Stand
Fuel Tank Caps	70.76	2	141.52	Fluids	Test Stand
Fuel Tank Adapters	22.37	2	44.74	Fluids	Test Stand

Solenoid Valves	59.95	5	299.75	Fluids	Test Stand
1in NPT Nipples	4.27	2	8.54	Fluids	Test Stand
Reducing Adapters	5.69	2	11.38	Fluids	Test Stand
1/4 NPT Nipples	12.99	3	38.97	Fluids	Test Stand
1/4 NPT Tee	12.99	6	77.94	Fluids	Test Stand

Joints						
PTFE Tape 1/4	3.66	2	7.32	Fluids	Test Stand	
PTFE Tape 3/2	16.26	1	16.26	Fluids	Test Stand	
F-F 1/8in connectors	5.2	4	20.8	Fluids	Test Stand	
1/8 in NPT Tee	5.61	4	22.44	Fluids	Test Stand	
90 Elbow NPT F	3.31	4	13.24	Fluids	Test Stand	
Check Valve 1/4 NPT	21.44	2	42.88	Fluids	Test Stand	
Straight Reducer	3.2	1	3.2	Fluids	Test Stand	
1/4 NPT Tee	13.16	3	39.48	Fluids	Test Stand	
1/4 NPT Small Nipples	2.55	6	15.3	Fluids	Test Stand	
CGA 580 Regulator	214.86	1	214.86	Fluids	Test Stand	
Nitrous Regulator	0	1	0	Fluids	Test Stand	
Aluminum Baseplate	104.53	1	104.53	Manufacturing	Test Stand	
Rolled Steel L-beams	0	8	0	Manufacturing	Test Stand	
Coated L-beams	0	10	0	Manufacturing	Test Stand	
Plexiglass Plates	0	6	0	Manufacturing	Test Stand	
Ratchet Straps	4.75	8	38	Manufacturing	Test Stand	
Bolts 100pk	17.24	1	17.24	Manufacturing	Test Stand	

Locknuts 100pk	7.2	1	7.2	Manufacturing	Test Stand
Load Cell	40	1	40	Systems	Test Stand
Prototyping Board	13.99	1	13.99	Systems	Test Stand
Load Cell Amplifier	8.29	1	8.29	Systems	Test Stand
22 AWG Wire	15.19	1	15.19	Systems	Test Stand
5V Relays	10.99	1	10.99	Systems	Test Stand
Pressure Transducers	15.23	6	91.38	Systems	Test Stand
Thermocouples	22	4	88	Systems	Test Stand
14 AWG Wire	19	1	19	Systems	Test Stand
Cat 5e Cable 1000ft	60	1	60	Systems	Test Stand
LiFePO4 Battery	33.59	1	33.59	Systems	Test Stand
LiFePO4 Charger	28.55	1	28.55	Systems	Test Stand
Heat Shrink Tubing	6.59	1	6.59	Systems	Test Stand
Screw Terminals	8.99	1	8.99	Systems	Test Stand
5 Ohm Resistors	6.99	1	6.99	Systems	Test Stand
Steel Wool	5	1	5	Systems	Test Stand

## **Design and Development Summary**

Throughout the course of this project, everyone on the RPU-1 team has learned a substantial amount about the design and fabrication of complex engineering projects.

In addition to the knowledge gained by committee leadership, we have also taught many committee members about the design process through hands-on involvement in simulation, material selection, coding, soldering, manufacturing, trade studies, and much more. As we navigate the intricate logistics of propellant transport, we are providing an easier path for future engineering teams to explore the viability of their designs in a safe manner. Overall, we hope that RPU-1 and its lineage equips future students with the level of experience we have gained developing it.